# We are IntechOpen, the world's leading publisher of Open Access books Built by scientists, for scientists

6,900
Open access books available

185,000
International authors and editors

200M
Downloads

Our authors are among the

154
Countries delivered to

TOP 1%
most cited scientists

12.2%
Contributors from top 500 universities




WEB OF SCIENCE™

Selection of our books indexed in the Book Citation Index in Web of Science™ Core Collection (BKCI)

## Interested in publishing with us?
## Contact book.department@intechopen.com

Numbers displayed above are based on latest data collected.
For more information visit www.intechopen.com



Chapter 2

# Dynamics of Droplets

Hossein Yahyazadeh and Mofid Gorji-Bandpy

Additional information is available at the end of the chapter

http://dx.doi.org/10.5772/61901

**Abstract**

Capturing non-Newtonian power-law drops by horizontal thin fibers with circular cross-section in a quiescent media can be studied in this chapter. The case is simulated using volume of fluid (VOF) method providing a notable reduction of a computational cost. Open source OpenFOAM software is applied to conduct the simulations. This model is an extension of the one developed earlier by Lorenceau, Clanet, and Quéré [1]. To validate the model, water drops affecting a fiber of radius 350μm were simulated and threshold drop radiuses were obtained regarding to the impact velocity. These results agreed well with the experimental data presented by Lorenceau et al. [1]. In the next step, non-Newtonian power-law drops landing on thin fiber of radius 350μm were simulated. The final goal of this study was to obtain the threshold velocity and radius of a drop that is completely captured by the fiber. Threshold radiuses for both shear-thinning and shear-thickening drops were obtained and compared with corresponding Newtonian drops. Results show that the threshold radius of drop increases in a fixed velocity as $n$, power-law index, increases. Furthermore, shear-thinning nature of the drop leads to instabilities in high Reynolds numbers (Re) as it influences the fiber.

**Keywords:** Impact, Wetting, Filtration, Non-Newtonian Drop, Power-Law Model

## 1. Introduction

The problem of the removal of aerosol particles from gas streams has become of increasing importance from the standpoint of public health and the recovery of valuable products. Technology of controlling the aerosol particles or improving the liquid phase of aerosol is very important in many industrial processes such as oil and petroleum, electronic, mining, and food, as well as waste products like noxious emission of aerosol in chemical plants. There are several ways for this purpose among which fibrous filters are more popular so that it is obvious to try to improve their efficiency. The efficiency of collection and the pressure drop are the most important practical considerations in the design of these fibrous filters [2]. Various

INTECH
open science | open minds

© 2017 The Author(s). Licensee InTech. This chapter is distributed under the terms of the Creative Commons Attribution License (http://creativecommons.org/licenses/by/3.0), which permits unrestricted use, distribution, and reproduction in any medium, provided the original work is properly cited.

experimental studies on liquid aerosol filtration have shown a filter clogging in several stages leading to a drainage stage with a constant pressure drop [3, 4]. Contal et al. [3] introduced four stages describing the clogging of fibrous filters by liquid droplets: In the first stage, the droplets impact the wet fibers. In the second stage, the amount of those droplets captured by fiber increases so that neighbor droplets coalesce. In the third stage, liquid shells form in the net that leads to a large increase of the pressure drop and to a dramatic decrease in the efficiency of the filter. Finally, there will be a pseudo-stationary state between the droplet collection and gravitational drainage of the liquid phase [1]. The first stage of clogging is studied in many researches experimentally. Patel et al. [5] investigated the drop breakup in a flow through fiber filters and the breakup probability for a drop. Hung and Yao [6] evaluated the impact of water droplets on a cylindrical object experimentally. Both these studies show that depending on the speed of the impacting droplets, the drops can be captured and broken into several pieces. Lorenceau et al. [1] investigated the threshold velocity and radius of drops captured by thin fibers. They have shown that the threshold impact velocity of drops decreases as the drop radius increases and vice versa. Following this study, Lorenceau et al. [7] investigated off-center impact of droplets on horizontal fibers.

Most of liquid droplets in aerosols produced in different industrial and natural processes show non-Newtonian behavior. Therefore, studying the phenomenon of impaction of a non-Newtonian droplet on thin fibers is of prime importance. All mentioned studies have been devoted to Newtonian fluids. Colliding of non-Newtonian droplets on thin fibers, to our knowledge, has not been investigated previously. However, colliding of non-Newtonian drops on flat plates is evaluated in some experimental and numerical studies. Haeri and Hashemabadi [8] studied spreading of power-law fluids on inclined plates both numerically and experimentally. Saïdi et al. [9] investigated experimentally the influence of yield stress on the fluid droplet impact control. Son and Kim [10] studied experimentally the spreading of inkjet droplet of non-Newtonian fluid on a solid surface with controlled contact angle at low Weber and Reynolds numbers. Kim and Baek [11] investigated the parameters that govern the impact dynamics of yield stress on the fluid droplets on solid surfaces.

In this chapter, we focus on the first stage of clogging and investigate the impaction of non-Newtonian power-law fluids on thin fibers. We aim to obtain the threshold radius of impacting droplets in different impact velocities. Effect of shear-thinning and shear-thickening behavior of droplets is evaluated and compared with corresponding Newtonian fluids. For this purpose, volume of fluid method is used and open source OpenFOAM software is applied for simulations.

The order of contents in this chapter is as follows: In Section 2 the governing equations and numerical methodology are given. Validation of the obtained results for Newtonian fluids in comparison with experimental observations presented by Lorenceau et al. [1] is provided in Section 3.1. A general description of the observations for non-Newtonian droplets captured by horizontal fiber is presented in Section 3.2, and the behavior of non-Newtonian drops affecting thin fibers is explained. Finally, a summary of the results and conclusions is provided.

http://dx.doi.org/10.5772/61901

## 2. Methodology

### 2.1. Volume of fluid method

Hirt and Nichols [12] demonstrated the volume of fluid (VOF) method and started a new trend in multiphase flow simulation. It relies on the definition of an indicator function $\gamma$. This function allows us to know whether one fluid or another occupies the cell, or a mix of both. In the conventional volume of fluid method [12], the transport equation for an indicator function $\gamma$, representing the volume fraction of one phase, is solved simultaneously with the continuity and momentum equations as follows:

$$\nabla.\mathbf{U} = 0 \tag{1}$$

$$\frac{\partial \gamma}{\partial t} + \nabla.\left(\mathbf{U}\gamma\right) = 0 \tag{2}$$

$$\frac{\partial\left(\rho\mathbf{U}\right)}{\partial t} + \nabla.\left(\rho\mathbf{U}\mathbf{U}\right) = -\nabla p + \nabla.\mathbf{T} + \rho\mathbf{f}_b \tag{3}$$

where $\mathbf{U}$ represents the velocity field shared by the two fluids throughout the flow domain, $\gamma$ is the phase fraction, $\mathbf{T}=2\mu\,\mathbf{S} - 2\mu\,(\nabla.\mathbf{U})\,\mathbf{I}/3$ is the deviatoric viscous stress tensor, with the mean rate of strain tensor $\mathbf{S}=0.5[\nabla\mathbf{U} + (\nabla\mathbf{U})^T]$ and $\mathbf{I}=\delta_{i,j}$, $\rho$ is density, $p$ is pressure, and $\mathbf{f}_b$ are body forces per unit mass. In VOF simulations, the latter forces include gravity and surface tension effects at the interface. The phase fraction $\gamma$ can take values within the range $0 \le \gamma \le 1$, with the values of zero and one corresponding to regions accommodating only one phase, for example, $\gamma=0$ for gas and $\gamma=1$ for liquid. Accordingly, gradients of the phase fraction are encountered only in the region of the interface. Two immiscible fluids are considered as one effective fluid throughout the domain, the physical properties of which are calculated as weighted averages based on the distribution of the liquid volume fraction, thus being equal to the properties of each fluid in their corresponding occupied regions and varying only across the interface:

$$\rho = \rho_1\,\gamma + \rho_g\left(1-\gamma\right) \tag{4}$$

$$\mu = \mu_1\,\gamma + \mu_g\left(1-\gamma\right) \tag{5}$$

where $\rho_l$ and $\rho_g$ are densities of liquid and gas, respectively.

In this study, a modified approach similar to the one proposed in [13] is used.

### 2.2. Power-law model

Generally, the form of the function relating $\tau_{xy}$ to shear rate $\dot{\gamma}$ is quite complicated. It has been found, however, that the two-parameter equation of state

$$\tau_{xy} = K\dot{\gamma}^{n} \tag{6}$$

is adequate for many non-Newtonian fluids [16], where $K$ is the fluid consistency coefficient and $n$ is power-law index. This is a well-known power-law model, which is used in this study.

### 2.3. Computational method

All computations are performed using the code OpenFOAM [17], an open source computational fluid dynamics (CFD) toolbox, utilizing a cell-center-based finite volume method on a fixed unstructured numerical grid and employing the solution procedure based on the pressure implicit with splitting of operators (PISO) algorithm for coupling between pressure and velocity in transient flows [18].

A grid spacing equal to 1/20 of the droplet radius was used to discretize the computational domain. The mesh size was determined based on a mesh refinement study in which the grid spacing was progressively decreased until further reductions made no significant change in the predicted droplet shape during the impact. Bussmann et al. [19] have provided a detailed description of such a mesh refinement study earlier. The mesh size was uniform throughout the computational domain, which included the droplet and fiber.

## 3. Results and discussion

### 3.1. Validation of the Solution

In this section, we present the results obtained for water droplets impacting a fiber of radius 350 μm. Physical properties of water are given in Table 1. Threshold radiuses of the droplets in different impact velocities are obtained and compared with those exhibited by Lorenceau et al. [1]. All obtained results are shown in Figure 1, which demonstrates the threshold radiuses in different impact velocities.

| $n$ | $\rho\ (kg/m^3)$ | $k\ (mPa \cdot s^n)$ | $\sigma\ (mN/m)$ | fluid |
|---|---|---|---|---|
| 1 | 1000 | 1 | 70 | water |

**Table 1.** Physical properties of fluids

http://dx.doi.org/10.5772/61901

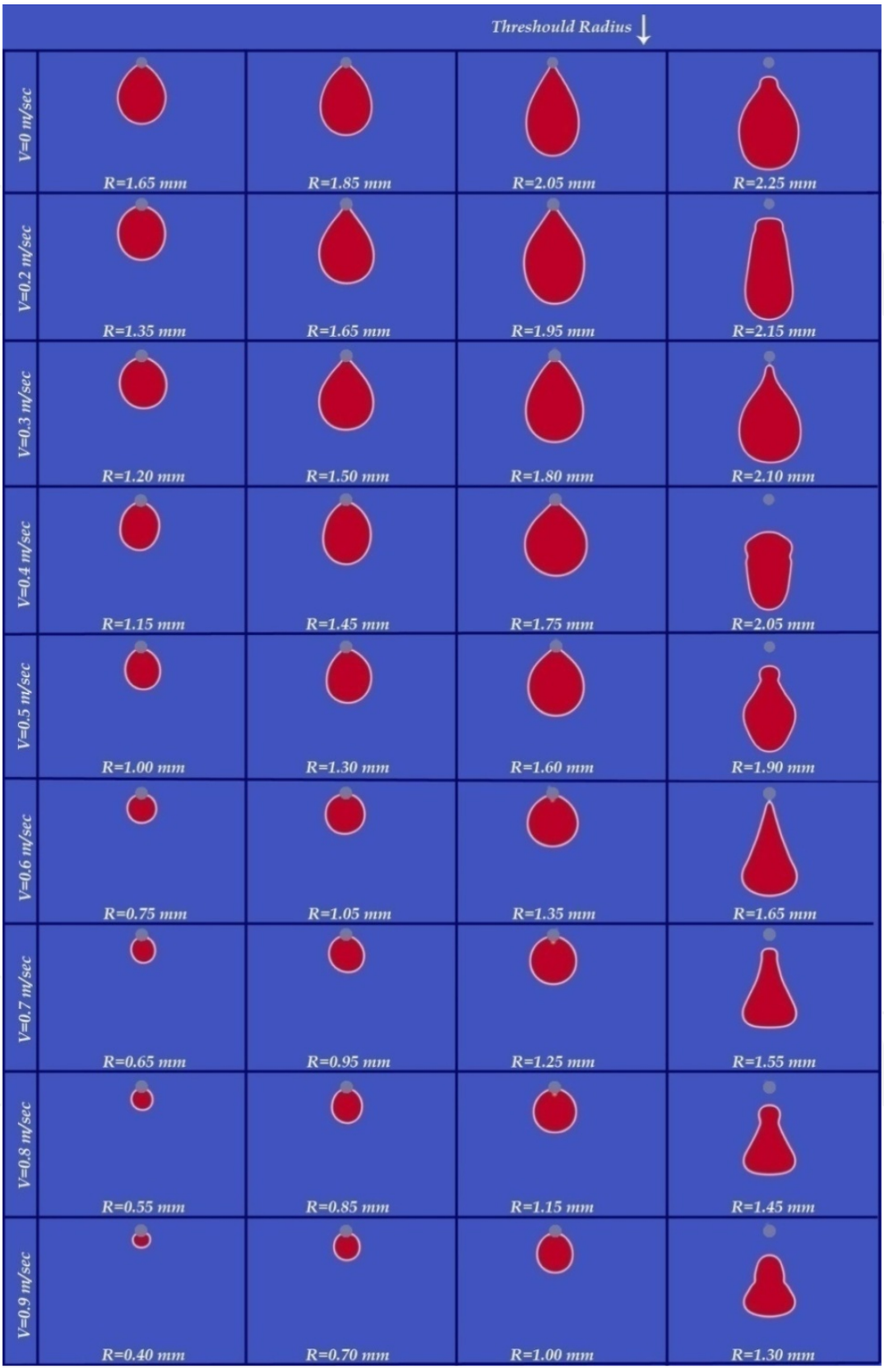



**Figure 1.** Threshold radiuses of the water droplets in different impact velocities

Defining $R_M$ as characteristic radius of the drop at zero impact velocity as follows:

$$R_M = 3^{1/3} b^{1/3} k^{-2/3} \tag{7}$$

where $k^{-1} = \sqrt{\sigma / \rho g}$ is the capillary length and $b$ is the radius of the fiber, and also characteristic velocity of the drop as:

$$U_M = \sqrt{4 g R_M} \tag{8}$$

Variation of the dimensionless threshold radius versus dimensionless impact velocity is plotted in Figure 2, which shows a good agreement with the experimental and theoretical data presented by Lorenceau et al. [1].

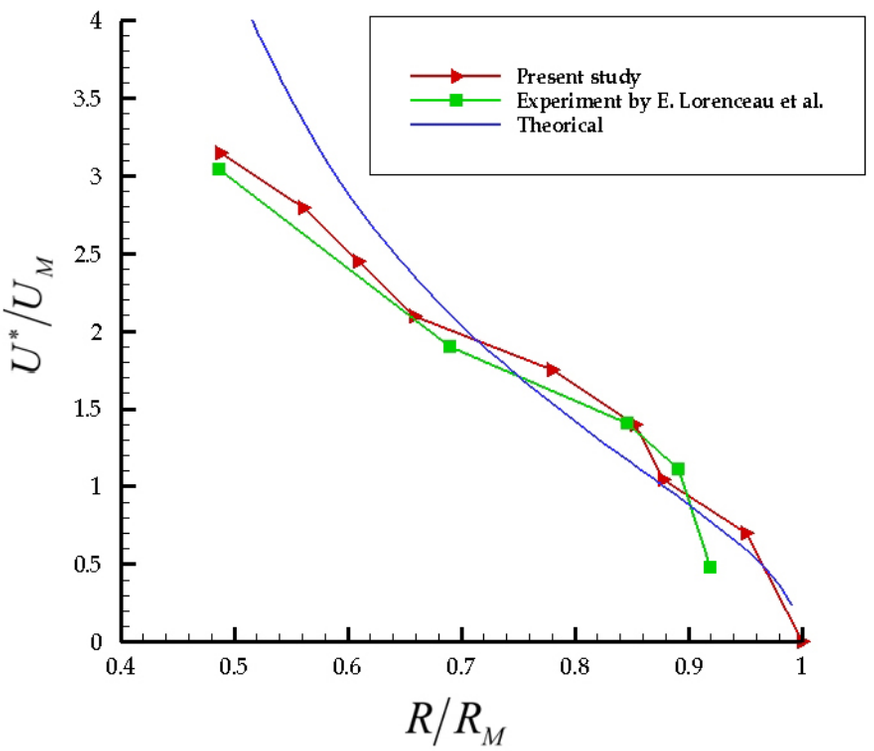



**Figure 2.** Comparison of the obtained results with experimental and theoretical data

Errors of the achieved results in comparison with experimental results of Lorenceau et al. (2004) are presented in Table 2.

| % Errors in comparison with theoretical data | % Errors in comparison with experimental data | $U/UM$ Theoretical data | $U/UM$ Experimental data | $U/U_M$ Present study | $R/R_M$ |
|---|---|---|---|---|---|
| 3.68 | 12.6 | 1.00 | 1.19 | 1.04 | 0.87 |
| 23 | 2.96 | 1.13 | 1.35 | 1.39 | 0.85 |
| 14.47 | 8.07 | 1.52 | 1.65 | 1.74 | 0.78 |
| 11.06 | 0.48 | 2.35 | 2.08 | 2.09 | 0.65 |
| 12.54 | 4.27 | 2.79 | 2.34 | 2.44 | 0.60 |
| 16.46 | 6.48 | 3.34 | 2.62 | 2.79 | 0.56 |
| 30.53 | 3.63 | 4.52 | 3.03 | 3.14 | 0.48 |

**Table 2.** Errors of the achieved results in comparison with the experimental and theoretical data

### 3.2. Results for non-newtonian droplets

Four forces, capillary, gravity, inertia, and viscosity, are important during the impaction of droplet to the fiber. Capillary and gravity forces are in contrast. While the weight of the drop tends to detach it from the fiber, surface tension is responsible for the sustentation. In order to analyze the dynamics of the capture of a drop by a fiber, viscous and inertia effects must be considered. Here again, those effects are antagonistic. While inertia tends to make the drop cross the fiber, viscous effects will induce a dissipation and can thus possibly stop the drop [1]. Effects of variation of viscosity were not investigated in the previous works. In order to investigate these effects, both shear-thinning and shear-thickening fluids will be considered.

At first, we present general observations of threshold radiuses at different velocities for shear-thinning droplets, $n<1$. For this purpose, physical properties of the fluid given in Table 1 were used except the power-law index, which is equal to 0.5. Figure 3 represents the threshold radiuses in different velocities for this type of droplet.

Next, we present our observations for the two kinds of shear-thickening droplets, $n$=1.5, 2, impacting the fiber which are shown in Figures 4 and 5.

Results show that, on the one hand, in shear-thinning drops, the threshold radius decreased in a fixed velocity in comparison with the corresponding Newtonian drops. Moreover, instabilities were observed during the impaction of the drop. This is because viscosity in shear-thinning fluids decreases as it has an inverse relation with shear rate. That is, as a shear-thinning droplet impacts a thin fiber, due to high shear rates, viscosity decreases in comparison with the corresponding Newtonian fluid, so that the viscosity force reduces (i.e., a force that helps the drop to stick on the fiber is reduced). Thus, in order to balance the antagonistic forces, drop size has to be decreased, which means the threshold radius has to be decreased. On the other hand, in the case where the drop is a shear-thickening fluid, the threshold radius increased in a fixed velocity in comparison with the corresponding Newtonian fluid, since the viscosity of shear-thickening fluids has a direct relation to the shear rate. It means that, viscosity increases as the drop impacts the fiber compared to Newtonian drops. Thereby, in shear-

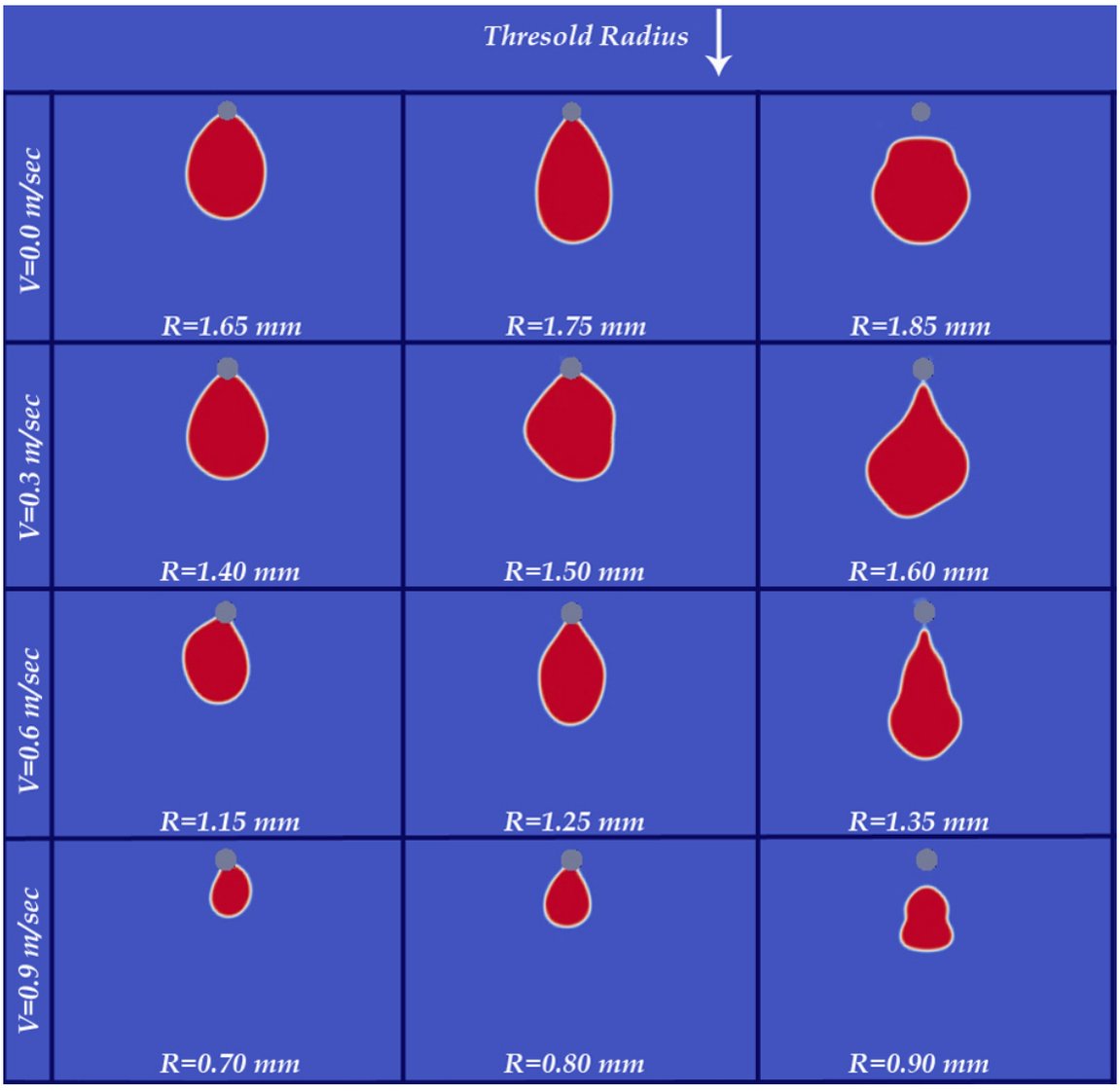



**Figure 3.** Threshold radiuses of the shear-thinning ($n$=0.5) droplets in different impact velocities

thickening drops, viscous forces increase and the drop's tendency to stick to the fiber increases. Therefore, the threshold drop size will also increase. This tendency is obvious in Figures 4 and 5. Threshold radius of Newtonian, shear-thinning and shear-thickening droplets versus impact velocity is plotted in Figure 6.

Figure 6 shows that the threshold radius will decrease generally with the increase of an impact velocity or vice versa. In shear-thinning droplets, viscosity has an inverse relation with shear rate, as mentioned before, so that it will decrease with the increase of impact velocity. It means inertia forces increase whereas viscosity forces decrease. That is why instabilities are observed in shear-thinning droplets impacting fiber at high speeds. The threshold radius of shear-thickening droplets, also, decreases with the increase of impact velocity. In shear-thickening droplets, although there is a direct relation between the viscosity and the shear rate, velocity increases with second power compared to capillary forces. That is, increase of inertia forces is

http://dx.doi.org/10.5772/61901

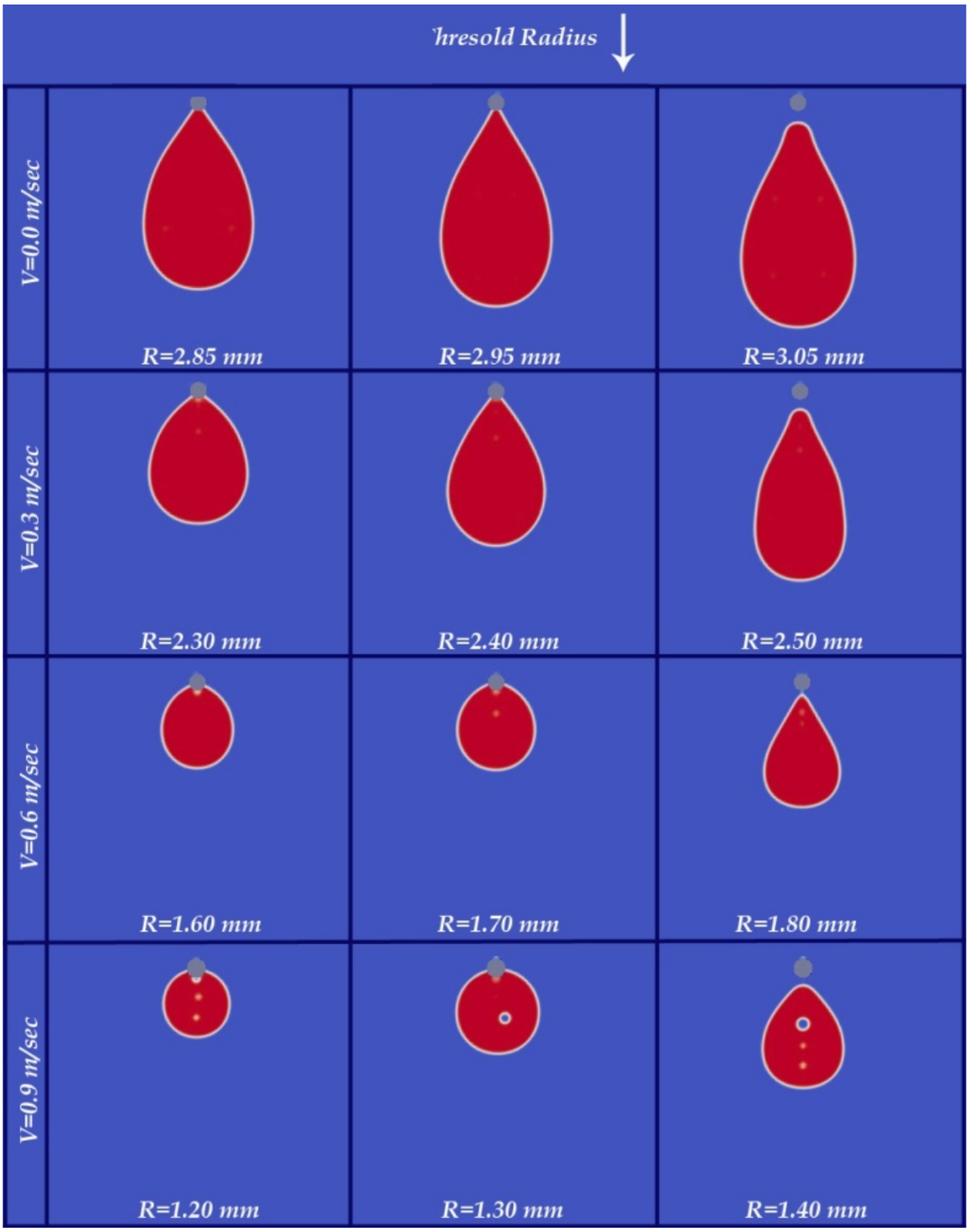



**Figure 4.** Threshold radiuses of the shear-thickening ($n$=1.5) droplets in different impact velocities

higher than increase of viscosity forces so that the threshold radius will decrease to make the drop stick to the fiber. However, in higher velocities, this rate will decrease as it can be seen in Figure 6. In other words, rate of the decreasing of threshold radius with the increasing of impact velocity will decrease due to high growth of shear rate.

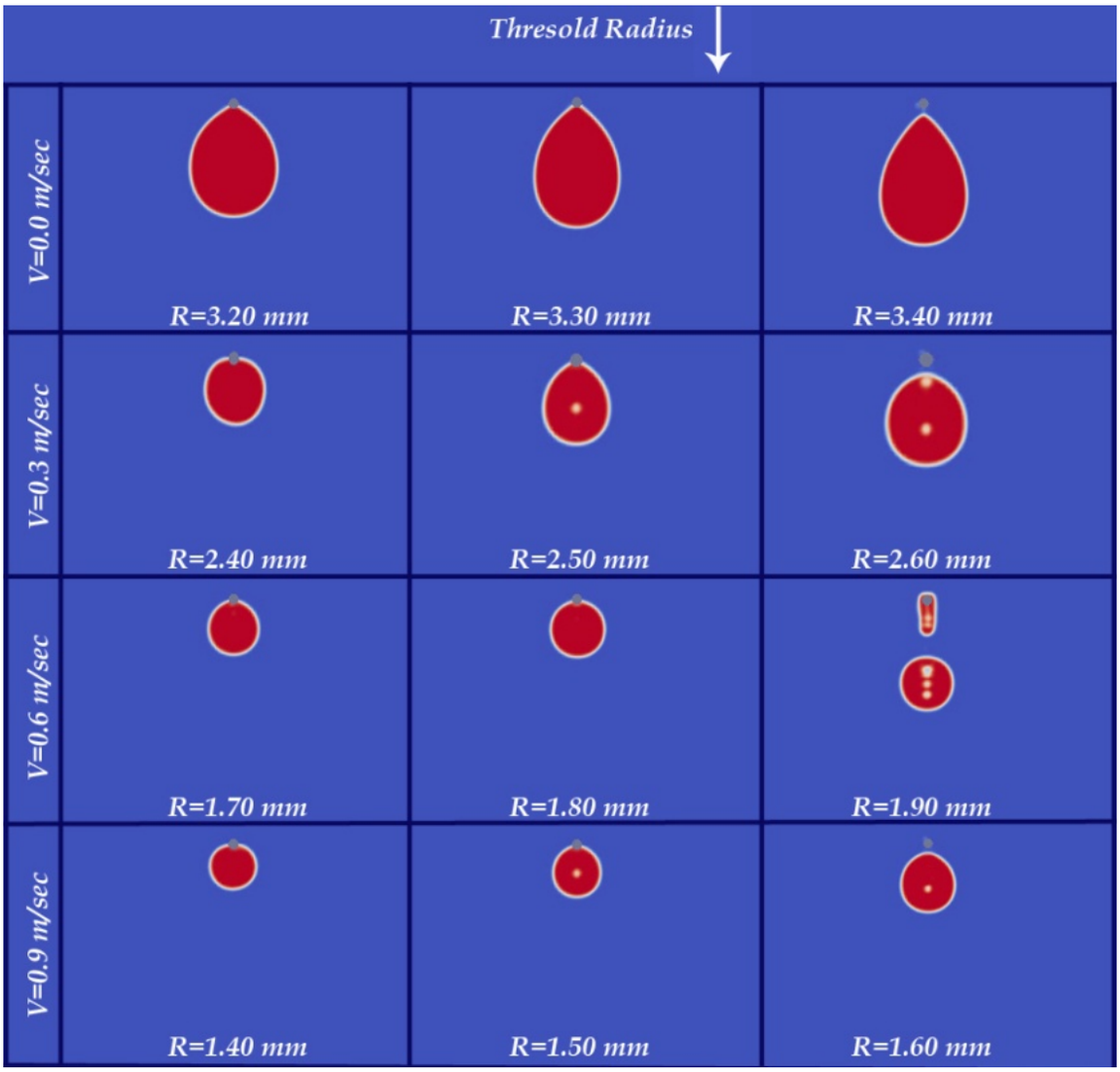



**Figure 5.** Threshold radiuses of the shear-thickening ($n$=2) droplets in different impact velocities

There are some general observations that are common to Newtonian and non-Newtonian fluids. For all kinds of fluids, the threshold radius of the droplet has a reverse relation with the impact velocity of the droplet. In all cases, at a fixed impact velocity, droplets with a radius greater than the threshold radius have passed the fiber without breakup, and drops with a radius lower than the threshold radius clung to the fiber entirely.

## 4. Conclusion

Impaction of non-Newtonian power-law droplet to the horizontal fiber of circular cross section is investigated in this study. Volume of fluid technique is employed, significantly reducing the computational cost. Outcomes are divided into three parts: First, it has been observed that the threshold radius of the droplets decreased with the increase of impact velocity for New-

http://dx.doi.org/10.5772/61901

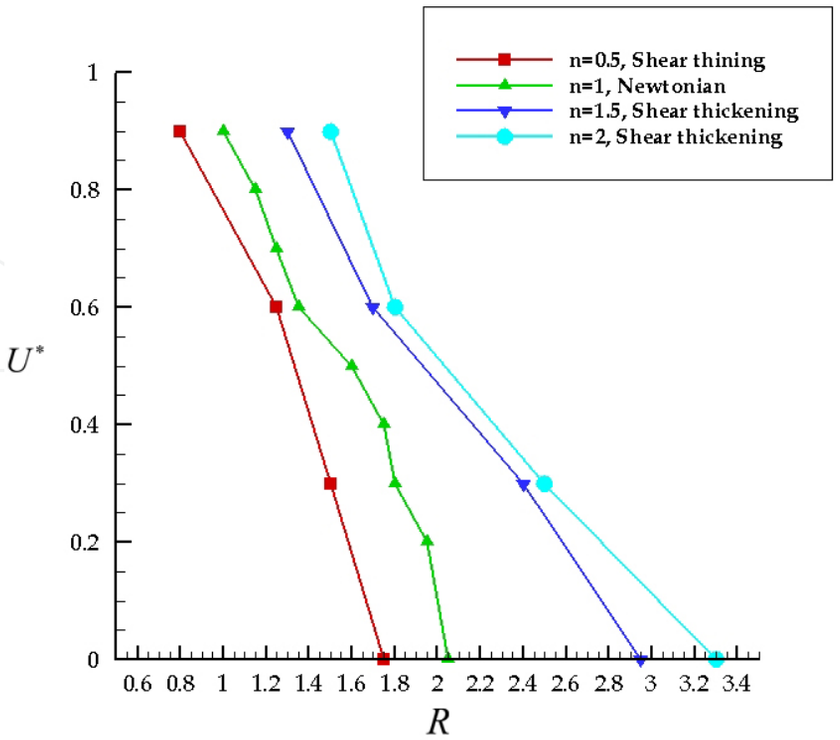



**Figure 6.** Threshold radiuses of droplets versus impact velocity for Newtonian, shear-thinning and shear-thickening fluids

tonian, shear-thinning and shear-thickening fluids, due to the growth of inertia forces versus viscosity and capillary forces. Second, instabilities have been observed in shear-thinning droplets at high impact velocities due to severe reduction of viscosity. Finally, in shear-thickening droplets, at high impact speeds, rate of reduction of threshold radius has decreased due to increase of the viscosity forces.

## Author details

Hossein Yahyazadeh and Mofid Gorji-Bandpy*

*Address all correspondence to: gorji@nit.ac.ir

Department of Mechanical Engineering, Babol University of Technology, Babol, Iran

## References

[1] É. Lorenceau, C. Clanet, D. Quéré, Capturing drops with a thin fiber, Journal of Colloid and Interface Science, vol. 279, 192–197, 2004.

[2] C.Y. Chenz, Filtration Of Aerosols By Fibrous Media,DA18-108-CML-4789 with the Chemical Corps, U.S. Army, Washington 25, D.C, March 6, 1955.

[3] P. Contal, J. Simao, D. Thomas, T. Frising, S. Call, J.C. Appert-Collin, D. Bemer, Clogging of fibre filters by submicron droplets. Phenomena and influence of operating conditions, Aerosol Science, vol. 35, 263–278, 2004.

[4] D.C. Walsh, J.I.T. Stenhouse, K.L. Scurrah, A. Graef, The effect of solid and liquid aerosol particle loading on fibrous filter material performance, Journal of Aerosol Science, vol. 27, 617–618, 1996.

[5] P. Patel, E. Shaqfeh, J.E. Butler, V. Cristini, J. Blawzdziewicz, M. Loewenberg, Drop breakup in the flow through fixed fiber beds: An experimental and computational investigation, Physics of Fluids, vol. 15, 1146, 2003.

[6] L.S. Hung, S.C. Yao, Experimental investigation of the impaction of water droplets on cylindrical objects, International Journal of Multiphase Flow, vol. 25, 1545–1559, 1999.

[7] E. Lorenceau, C. Clanet, D. Quéré, M. Vignes-Adler, Off-centre impact on a horizontal fibre, European Physical Journal Special Topics, vol. 166, 3–6, 2009.

[8] S. Haeri, S.H. Hashemabadi, Three dimensional CFD simulation and experimental study of power law fluid spreading on inclined plates, International Communications in Heat and Mass Transfer, vol. 35, 1041–1047, 2008.

[9] Alireza Saïdi, Céline Martin, Albert Magnin, Influence of yield stress on the fluid droplet impact control, Journal of Non-Newtonian Fluid Mechanics, vol. 165, Issues 11–12, 596–606, 2010.

[10] Yangsoo Son, Chongyoup Kim, Spreading of inkjet droplet of non-Newtonian fluid on solid surface with controlled contact angle at low Weber and Reynolds numbers, Journal of Non-Newtonian Fluid Mechanics, vol. 162, Issues 1–3, 78–87, 2009.

[11] Eunjeong Kim, Jehyun Baek, Numerical study of the parameters governing the impact dynamics of yield-stress fluid droplets on a solid surface, Journal of Non-Newtonian Fluid Mechanics, vol. 173–174, 62–71, 2012.

[12] C.W. Hirt, B.D. Nichols, Volume of fluid (VOF) method for the dynamics of free boundaries, Journal of Computational Physics, vol. 39, 201–225, 1981.

[13] H. Rusche, Computational Fluid Dynamics of Dispersed Two-Phase Flows at High Phase Fractions, Imperial College of Science, Technology and Medicine, Ph.D. thesis, 2002.

[14] G. Černe, S. Petelin, I. Tiselj, Coupling of the interface tracking and the two-fluid models for the simulation of incompressible two-phase flow, Journal of Computational Physics, vol. 171, 776–804, 2001.

[15] J.U. Brackbill, D. B. Kothe, C. Zemach, A continuum method for modeling surface tension, Journal of Computational Physics, vol. 100, 335–354, 1992.

[16] Rohit Aiyalur Shankaran, Numerical Simulation Of Flow Of Shear-Thinning Fluids in Corrugated Channels, M.Sc. thesis, Texas A&M University, December 2007.

[17] H.G. Weller, G. Tabor, H. Jasak, C. Fureby, A tensorial approach to computational continuum mechanics using object orientated techniques, Computers in Physics, vol. 12, 620–631, 1998.

[18] R.I. Issa, Solution of the implicitly discretised fluid flow equations by operator-splitting, Journal of Computational Physics, vol. 62, 40–65, 1986.

[19] M. Bussmann, J. Mostaghimi, S. Chandra, On a three-dimensional volume tracking model of droplet impact, Physics of Fluids, vol. 11, 1406–1417, 1999.

IntechOpen

IntechOpen

IntechOpen